STUDY OF NEGATIVE THERMAL EXPANSION IN HALF HEUSLER MARTENSITE

A Dissertation for

PHY-651 Dissertation

Credits: 8

Submitted in partial fulfillment of Masters Degree

M.Sc in Physics (Solid State Physics)

Goa University

in the subject of Physics

by

JERIZA PEREIRA
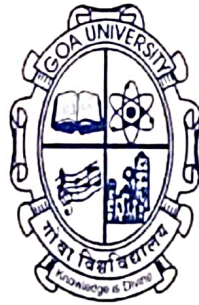
Roll number: 22P0430013

ABC ID: 864-502-941-778

PRN: 201905883

Under the supervision of

Dr. K.R.S Priolkar

School Of Physical and Applied Science

Physics discipline

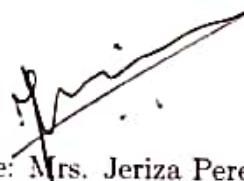**Goa University**

May 2024

Examined by:

Seal of the School

i

DECLARATION BY STUDENT

I hereby declare that the data presented in this Dissertation / Internship report entitled. "Study of negative thermal expansion in half heusler martensite" is based on the results of investigations carried out by me in the Physics Discipline at the School of Physical and Applied Sciences, Goa University under the Supervision of Dr. Kaustubh R. Priolkar and the same has not been submitted elsewhere for the award of a degree or diploma by me. Further, I understand that Goa University or its authorities will be not be responsible for the correctness of observations / experimental or other findings given the dissertation.

I hereby authorize the University authorities to upload this dissertation on the dissertation repository or anywhere else as the UGC regulations demand and make it available to any one as needed.

Name: Mrs. Jeriza Pereira

Roll no: 22P0430013

Discipline: Physics

School of Physical and Applied Sciences

Date: May 2024

Place: Goa University

COMPLETION CERTIFICATE

This is to certify that the dissertation / internship report "Study of negative thermal expansion in half heusler martensite" is a bonafide work carried out by Mrs. Jeriza Pereira under my supervision in partial fulfilment of the requirements for the award of the degree of M.Sc in Physics at the School of Physical and Applied Sciences, Goa University.

Date:

Kaushbh R.S. Priolkar

Date: 06 May 2024

Place: Goa University

School stamp

<u>ACKNOWLEDGMENTS</u>

ABSTRACT

This report entails the study of negative thermal expansion on a half heusler martensite, specifically $MnCoGe$. It is aimed at understanding the structural and magnetic properties of $MnCoGe$ when Sn is substituted in stoichiometric amounts in Ge site. For $MnCoGe_{1-x}Sn_x$ $x = 0.075$ and $x = 0.1$ we observe a secondary transition below the normal magnetic ordering temperature. This transition is accompanied by the change in the coefficient of thermal expansion. $MnCoGe_{0.925}Sn_{0.075}$ has a negative coefficient of thermal expansion $\alpha_1 = -2.77 \times 10^{-6}$ from 80K to 110K and later has $\alpha_2 = 0.305 \times 10^{-6}$ for temperatures above 110K. $MnCoGe_{0.9}Sn_{0.1}$ sample has $\alpha_1 = -9.47 \times 10^{-6}$ between 75-120K and has $\alpha_2 = 2.35 \times 10^{-6}$ between 120K to 300K. These alloys however do not show structural transformation at room temperature. Further study on the nature of the low temperature transitions is an interest to be further pursued.

Contents

List of Tables

List of Figures

Chapter 1

Introduction

1.1 Martensitic transformation

Ferroic materials are systems that experience a change in symmetry at specific temperature or pressure thresholds known as phase transitions. A phase transition is described as a thermodynamic change in a homogeneous system due to external conditions. The transition may display as spontaneous electric polarization, magnetic polarization, or a structural distortion, which classifies them into three primary types: Ferromagnetic, ferroelectric and ferroelastic.

Ferroelastic materials undergo elastic and structural transitions. Elastic transformation effects present as lattice distortions like change in shape and volume. Structural transitions involve changes in the material's crystal structure or phase due to the application of external factors like application of stress or lowering of temperature. When such a transformation occurs diffusionlessly without displacement of atoms it is called as a martensitic transformation. It is a reversible phase transformation from a parent austenite (P phase) to a martensite (M phase) and vice versa. The cooling transformation from the high temperature austenitic phase to the low temperature martensitic phase begins at the martensitic start temperature (M_s) and a martensite is formed at a temperature known as martensitic finish temperature (M_f). Similarly on reversing the temperature a reverse transformation begins. This starts at the austenitic start

1
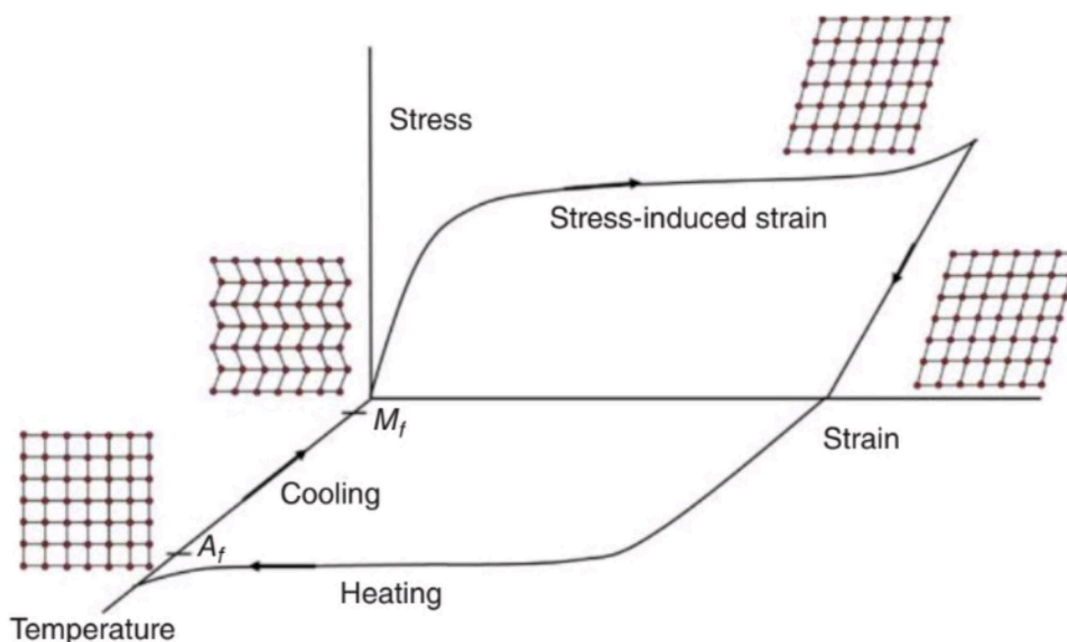
Figure 1.1: Martensitic Transformation [1]

temperature (A_s) and ends at the austenitic finish temperature (M_f) (Fig.2.8).

A martensitic transformation is a disorder-order transition and involves the reorientation of the strain vectors in solid, and involves no change in the composition. Hence it can be characterized by the non-displacive, diffusionless and shear type movement of atoms. This movement induces spontaneous distortion in an initially undistorted lattice with high symmetry, leading to the formation of a low symmetry phase known as martensite. The shearing of the crystal lattice occurs along specific crystallographic directions resulting in a change in the material's microstructure. The boundary between these two structures is called a habit plane. It acts as an interface between the parent structure and the transformed martensitic structure.

The cooperated rearrangement of atoms involves the change in shape. This shape change however is restricted by the surrounding matrix. This results in a twinning in the martensite. As the lattice undergoes the martensitic transformation shear strains lead to the formation of twin boundaries in the crystal. These twin boundaries are

regions where the crystal lattice is mirrored or rotated with respect to the surrounding lattice. They can have different orientations, known as varients, depending on the crystal structure and transformation mechanism. If a crystal structure contains different varients it is a twinned martensite[3, 2, 4]. On further application of stress these varients reorient themselves such that one orientation dominates. These are called detwinned martensite. The twinning and detwinning process on the application of load is called shape memory effect (SME).

1.2 Properties of Martensites

1.2.1 Shape Memory Alloys

One Way Shape Memory Effect

The principle of Shape Memory Alloys (SMAs) revolves around their ability to undergo reversible martensitic transformations, wherein they can "remember" and recover their original shape after deformation. SMAs are typically composed of a combination of metals, commonly nickel, titanium, and copper, with specific atomic arrangements that facilitate the martensitic transformation. At low temperatures, SMAs are in the martensitic phase, characterized by a lower symmetry crystal structure. When subjected to certain stimuli, such as temperature or stress, SMAs can undergo a reversible transformation from martensite to austenite phase and thereby recover their shape[2]. when austenite cools below certain temperatures (M_s and M_f), it transforms into twinned martensite. If the twinned martensite experiences high stress it starts to change shape, favoring some orientations over others. This transformation allows the material to accommodate strains by storing elastic energy. This reorientation happens at a stress level much lower than what would cause permanent deformation. The complete reorientation, called detwinning. The material can then be unloaded and it keeps the new shape. When heated, it transforms back to austenite. If no permanent deformation occurred during detwinning, the material regains its original shape. The strain recovered during this transformation is called transformation strain. The warming-cooling cycle

can repeat. This process is known as the one-way shape memory effect (SME) because shape recovery only happens during heating after detwinning due to mechanical stress. When the SMA is subjected to mechanical stress, it undergoes a martensitic transformation. Upon unloading the applied stress, the material reverts back to its original shape as it returns to the austenite phase, releasing the stored energy. A well-studied material that shows these properties is Nitinol.[5]

Two Way Shape Memory Effect

The Two-Way Shape Memory Effect (TWSME) allows a shape memory alloy (SMA) to remember and recover two different shapes alternately, depending on the temperature. TWSME occurs in Shape Memory Alloys (SMA) when they undergo cyclic thermal loading without any applied mechanical stress. The TWSME can be observed in materials which have undergone repeated thermo-mechanical cycling along a specific loading and unloading path until the material stabilizes in its response and the inelastic strain reaches a saturation point. In the initial cycles, upon heating, only a partial recovery of the strain from cooling is observed, leaving behind some permanent strain. With successive cycles, this additional permanent strain gradually decreases until it reaches a point where further accumulation ceases. During the warming cycle, the SMA returns to its original shape, while during the cooling cycle, it can revert to a previously defined shape. Repetition along a loading path for a large number of cycles can induce changes in the microstructure, creating defects that induce a residual internal stress state. This internal stress state allows the material to exhibit the TWSME behavior by favoring the formation of preferred martensitic variants during cooling in the absence of external loads [2].

1.2.2 Magnetic Shape Memory Alloys

Let us try to understand MSMA using an example. $NiMnGa$ is a type of shape memory alloy (SMA) that has the ability to undergo reversible shape changes in response to external stimuli such as temperature or magnetic fields. $NiMnGa$ alloys are the most widely studied Magnetic Shape Memory Alloys (MSMAs). These alloys were first reported to exhibit martensitic transformations in 1984, but the possibility of a magnetic field-controlled shape memory effect in these elements was suggested much later. In a martensitic phase transformation some of $Ni-Mn-Ga$ alloys transform to a five-layered modulated tetragonal structure (5M), which can show a large magnetic-field-induced strain (MFIS) of 0.2%–6%. This is referred to as the magnetic shape memory effect (MSME) is due to the rearrangement of martensitic twin variants in the magnetic field [6, 7]. The crystal structure of the martensitic Ni-Mn-Ga alloys is strongly influenced by the composition. The parent phase of $NiMnGa$ is generally a cubic Heusler-type structure, however the martensite structures can vary. The martensitic structures may include nonmodulated tetragonal (T), seven-layered modulated approximately orthorhombic (7M), or five-layered modulated approximately tetragonal forms. A combination of different martensite types may also be present. In alloys with a 5M martensite structure the easy axis of magnetization in martensite aligns with the shortest crystallographic axis. As the alloy transitions from the cubic parent phase to the martensitic structure during cooling, twins accommodate the strain generated in the transformation process. These twins can possess internal substructures or domains. Among these variants, the one aligned with the applied magnetic field begins to dominate. When these alloys are subjected to a magnetic field, the martensitic variants with a specific orientation of the magnetic moment (or easy magnetization axis) tend to grow at the expense of others due to the magnetic energy difference between them. As a result, the material changes its shape, exhibiting strain along the direction of the applied magnetic field. This forms the basis of the mechanics of Magnetic Shape Memory Effect (MSME) [7].

1.2.3 Superelasticity

In addition to the SME, SMAs exhibit superelastic behavior,sometimes also known as pseudoelasticity. Superelasticity (SE) refers to the ability of the material to undergo large reversible deformations without permanent damage, even beyond the elastic limit, often up to 8-10% strain. This is made possible by a reversible phase transformation within the material's crystal structure. Superelastic behavior of shape memory alloys (SMAs) happens when stress-induced transformation occurs, generating strain during loading and recovering it upon unloading at temperatures above a certain point (Af) [8, 9].

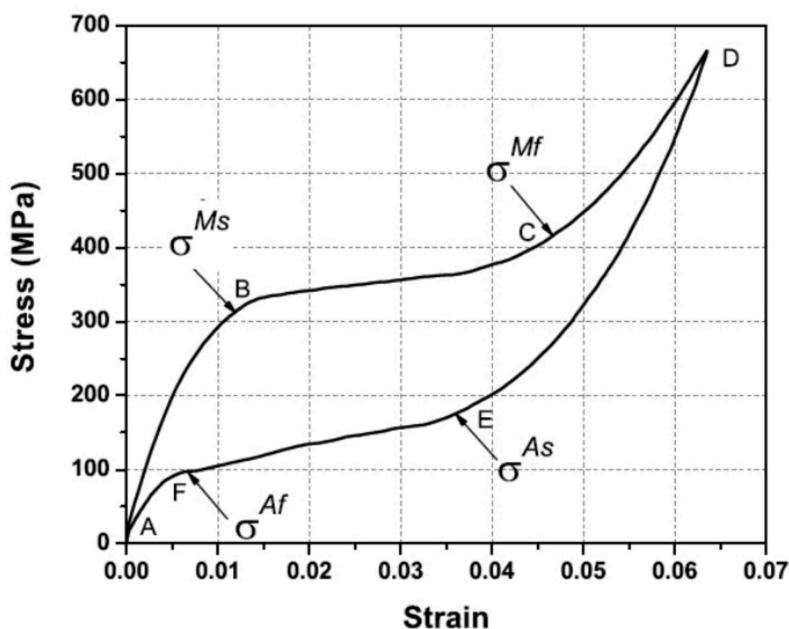Figure 1.2: SMA superelastic loading cycle [2]

At low stress and temperatures above A_f, when a mechanical load is applied, the parent phase (austenite) undergoes elastic loading shown in figure1.2 as path A-B. On increasing the load we reach the stress induced martensitic start temperature $\sigma^M s$. This is accompanied by the generation of large inelastic strains as shown in the stress-

strain diagram (S-S diagram). The transformation proceeds B-C on further increasing the load, until we reach the martensitic finish temperature, indicating the end of the transformation. Any subsequent increase in the stress causes no further transformation and causes elastic deformation indicated by path from C-D. When the stress is released gradually by unloading, the martensite elastically unloads. At point E the martensite to revert to austenite as stress reaches $\sigma^A s$. The process is accompanied by the recovery of the strain. The end of the transformation back into austenite is denoted by path E-F. The material then elastically unloads to A. The hysteresis observed in the S-S graph denotes the energy loss during the forward and reverse martensitic transformation [2].

1.2.4 Magnetocaloric Effect

Martensitic materials demonstrate a strong interconnection between their magnetic and structural transitions, a phenomenon termed magnetostructural coupling. This coupling emerges from the interplay among the electronic, magnetic, and lattice characteristics within the material. A key aspect of this coupling is its role in the magnetocaloric effect, enabling the magnetic field to govern structural phase transformations.

The magnetocaloric effect in martensitic materials is the capacity to initiate phase transitions through the application of a magnetic field. In these materials, the magnetostructural coupling allows the magnetic field to influence structural phase changes, thereby altering thermodynamic properties like entropy and temperature. When a magnetic field interacts with a martensitic material, the alignment of magnetic moments generates a force capable of modulating the structural phase transition. Consequently, this magnetic field-induced phase transformation generates alterations in the material's volume, shape, and other physical attributes. This shift in entropy, resulting from the magnetic field-induced phase transition, can produce either a cooling or heating effect, known as the magnetocaloric effect. This effect forms the basis for various applications in magnetic refrigeration and energy conversion.

Martensitic alloys such as $NiMnGa$ showcase remarkable magnetocaloric properties owing to their robust magnetostructural coupling. These materials exhibit substantial

changes in entropy induced by magnetic fields, thereby causing significant temperature fluctuations upon the application or removal of magnetic fields [10].

In martensitic alloys, the magnetocaloric effect is typically evaluated through parameters such as adiabatic temperature change, isothermal entropy change, and relative cooling power. These properties are contingent upon the material's specific composition, microstructure, magnetic field strength, and temperature range. Leveraging the magnetic-field-induced phase transitions in these materials enables the creation of efficient and eco-friendly cooling cycles, offering a sustainable approach to refrigerating and air-conditioning spaces.

The magnetostructural coupling in martensites can give rise to a plethora of intriguing phenomena, including magnetic-field-induced shape memory effects, giant magnetoresistance, and substantial magnetocaloric effects [11].

1.3 *MnCoGe*

The $MM'X$ (where M, M' − transition metals and $X - Si, Ge, Sn$) compounds have recently piqued the interest of scholars due to their megneto-responsive properties. One such compound is stoichiometric $MnCoGe$. $MnCoGe$ has a Ni_2In-type hexagonal structure at higher temperatures (P phase) and a $TiNiSi$-type orthorhombic structure at lower temperatures (M phase). The martensitic transformation temperature (T_m) where this structural transition from auestinite to martensite occurs for $MnCoGe$ is reported to be about $420K$ [11]. The change in the structure is accompanied by the change in lattice parameters. The orthogonal structure has lattice parameters derived as $a = 5.918\text{Å}, b = 3.827\text{Å}, c = 7.050\text{Å}$ and the volume is $V = 159.7\text{Å}3$. The lattice parameters for the hexagonal phase is reported to be $a = 4.087\text{Å}, c = 5.288\text{Å}$ and with volume $V = 76.48\text{Å}$ [12]. The relation for the mentioned parameters is given as: $a_{orth} \approx C_{hex}, b_{orth} \approx a_{hex}, \frac{c_{orth}}{\sqrt{3}} \approx c_{hex}$ and the volume $\frac{V_{orth}}{2} \approx V_{hex}$.

The Curie temperature T_C for orthorhombic martensite is $355K$. At this temperature the martensite undergoes magnetic ordering and transitions from a paramagnetic ground state to a ferromagnetic state [13]. The two transitions are summarised in the

diagram given below

Figure 1.3: Equation explaining the transitions in $MnCoGe$

Chapter 2

Experimental Techniques

In this chapter we shall go over the experimental techniques used for the preparation and characterization of this sample. The alloys were synthesised using arc melting technique and the crystal structure of the sample was determined using x-ray diffraction. This chapter also describes the DSC and four probe resistivity experiments that were conducted to study the transport properties. DMA was used for determining the mechanical characteristics of the sample and to prove the existence of glassy nature of the sample.

2.1 Sample Preparation

Manganese pieces (99.99% purity) were used. The pieces were weighed to the required weight and 1% extra was taken. It was then cleaned first with metal cleaner and then IPA. Five cycles of cleaning with metal cleaner were performed in the ultrasonicator of 15 minutes each. Manganese was cleaned till the pieces appeared to be polished and shinny. The pieces were finally cleaned with acetone before the melt. It was melted to form an Mn bead. This bead was crushed and weighed for sample preparation. Cobalt was cut from a cobalt block of 99.99% purity. The cobalt piece was hand cut and other elemental weights were adjusted accordingly. Cobalt was also cleaned prior to the melt. It underwent one cycle with metal cleaner of 5 minutes and then with acetone.

Germanium was cut directly from a block and weights were taken according to the requirements. Malleable Tin shots of 99.99% purity were pounded in a mortar-pestle into thin sheets. These sheets were then cut to adjust the weights.

- $MnCoGe$

Element	Required weight	Actual weight
Mn	0.4871	0.4873
Co	0.5225	0.5227
Ge	0.64406	0.6445

$$\text{Weight before melt} = 1.6545$$
$$\text{Weight after melt} = 1.6389$$
$$\text{weight loss} = \frac{1.6545 - 1.6389}{1.6545} \times 100$$
$$= 0.94\%$$

- $MnCoGe_{0.925}Sn_{0.075}$

Element	Required weight	Actual weight
Mn	0.5446	0.5446
Co	0.5842	0.5842
Ge	0.6659	0.6663
Sn	0.0881	0.0882

$$\text{Weight before melt} = 1.8833$$

$$\text{Weight after melt} = 1.820$$

$$\text{weight loss} = \frac{1.8833 - 1.8620}{1.8833} \times 100$$

$$= 1.12\%$$

- $MnCoGe_{0.9}Sn_{0.1}$

Element	Required weight	Actual weight
Mn	0.5318	0.5320
Co	0.5705	0.5705
Ge	0.6329	0.6333
Sn	0.1149	0.1150

$$\text{Weight before melt} = 1.8508$$

$$\text{Weight after melt} = 1.8333$$

$$\text{weight loss} = \frac{1.8508 - 1.8333}{1.8508} \times 100$$

$$= 0.94\%$$

This sample was synthesised via the Arc melting process in the *Centorr* arc furnace in an argon atmosphere (3 in Hg). The alloy bead was flipped and remelted three times to ensure homogeneity of the sample. Current was set at 75A and vacuum was recorded at 18 in Hg. The prepared samples were then vacuum sealed ($\sim 10^4$ mm of Hg) in a quartz tube. The alloys were cut using a low speed diamond cutter. Pieces of the required measurements were cut and powerded for the necessary characterisation. The MnCoGe alloys were annealed at 850°C for five days and furnace cooled to room temperature.

Figure 2.1: *Centorr* Arc Furnace and sample placed in the crucible of the furnace

Figure 2.2: Sample sealing procedure and sealed sample before annealing

Figure 2.3: Two-zone furnace used for annealing and annealed sample

2.2 X-ray Diffraction

Room temperature X-ray diffraction experiments were conducted using a Rigaku diffractometer with $M_o\,K\alpha$ radiation ($\lambda = 0.70926$ Å) at the School of Physical and Applied Sciences, Goa University. The measurements were taken from $20 \leq 2\theta \leq 100$ at room temperature. The data is then annalysed using LeBail method on Fullprof softwhere. X-ray diffraction is used to study the atomic and molecular structure of materials. X-ray diffraction is based on the interaction of X-rays with the crystal lattice of a material, we utilize the wave nature of X-rays to understand the periodic arrangement of atoms in crystalline materials. The wavelength of these X-rays are comparable to atomic spacings. When a beam of X-rays is directed at a crystalline sample, the X-rays are diffracted by the regularly spaced atoms within the crystal lattice. The principle governing this is given by Braggs law.

$$2d\sin(\theta) = n\lambda$$

14

d is the spacing between atomic planes in the crystal lattice.

θ is the angle of incidence or diffraction.

n is an integer representing the order of diffraction.

λ is the wavelength of the incident X-rays.

When X-rays interact with a crystal lattice, they produce a diffraction pattern consisting of bright spots or peaks. These peaks correspond to constructive interference. According to Bragg's law, constructive interference occurs when the path difference between waves scattered by adjacent atomic planes is equal to an integer multiple of the wavelength of the X-rays. By plotting the angles and intensities of the diffraction peaks in the pattern, we can find atomic arrangement within the crystal lattice, this includes atomic spacing and symmetry of the crystal structure[14].

Figure 2.4: Rigaku x-ray diffractometer

2.3 Electrical Resistivity Measurements

Figure 2.5: Electrical Resistivity Set-up

Essentially, the study of resistivity is done to understand the electrical conductivity behavior and properties of the material. Different materials display distinct resistive nature hence resistivity helps in categorizing the materials based on the atomic and molecular structures, defects, dopants and their dependence on temperature. The method we shall discuss here is the four probe resistivity method that is useful in measuring low resistivity in single crystals. The experiment was performed on a rectangular piece of sample of uniform surface area between the temperature range of $50 - 400°C$ on a D.C. four probe setup in a closed cycle refrigerator (CCR).

A typical four probe resistivity measurement set-up[15] consists of four probes on the flat surface of the sample. Current is passed through the outer electrodes through a direct current source while the the inner electrodes measure the potential. We then vary the temperature and measure the voltage V for a set current I of 10mA. We can
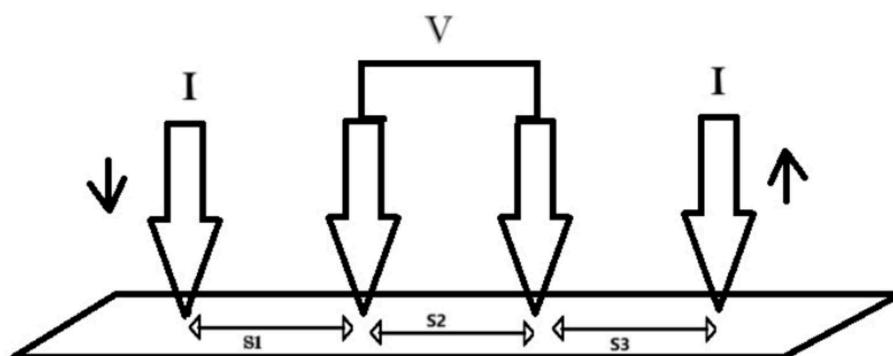
16

Figure 2.6: Four probe resistivity

then calculate the resistance R of the sample using ohm's law:

$$V = I \times R$$

Further we calculate the resistivity ρ of the sample using the formula:

$$\rho = \frac{R \times l}{A}$$

Where l and A is the length and area of the rectangular sample respectively.

2.4 Thermal Analysis

2.4.1 DSC

Differential Scanning Calorimetry (DSC) mearsurements were done on a Shimadzu DSC-60. The temperature range chosen was from $250 - 450K$ with approximately 9mg samples of each alloy securely crimped within aluminum pans. Heating and cooling cycles were recorded at a rate of 5°per min.

Differential Scanning Calorimetry (DSC) mearsurements involve measuring the heat flow (or heat capacity) of a sample as it undergoes changes in temperature. The DSC typically contains two pans - one for the sample and the other for a reference material. The DSC gradually heats or cools the sample and reference pans ensuring that both

pans are subjected to the same temperature conditions throughout the experiment at a controlled rate. As the sample undergoes physical or chemical changes, it either absorbs or releases heat. The DSC measures the temperature difference between the sample and reference pans, which reflects the amount of heat absorbed or released by the sample compared to the reference material. The difference in temperature between the two is recorded as a dip or a peak in the plot of heat flow as a function of time or temperature. This calorimetric analysis allows for the study of thermal behavior of materials like enthalpy changes, phase transitions and reaction kinetics.

Figure 2.7: Differential Scanning Calorimetry (DSC)- Shimadzu DSC-60

2.4.2 Thermal Expansion

Thermal expansion: Thermal expansion is the ability of the material by which materials vary in size or volume when exposed to different temperatures. This phenomenon occurs due to the increased kinetic energy of the atoms and molecules within the ma-

terial.

Linear Expansion: In solids, such as metals, the most common form of thermal expansion is linear expansion, where the material expands along its length. This can be quantified by the coefficient of linear expansion, denoted by α, which measures the fractional increase in length per degree of temperature rise.

Volumetric Expansion: Some materials, such as liquids and gases, undergo volumetric expansion, where they expand in all directions. This is measured by the coefficient of volume expansion, denoted by β, which represents the fractional increase in volume per degree of temperature rise.[16]

$$\Delta L = L_0 \alpha \Delta T$$

Where:

ΔL = Change in length

L_0 = Initial length

α = Coefficient of linear expansion

ΔT = Change in temperature

The equation demonstrates the linear expansion formula, showing how the change in length (ΔL) is proportional to the initial length (L_0), the coefficient of linear expansion (α), and the change in temperature (ΔT).

At the core of thermal expansion lies the atomic and molecular structure of materials. When heat is added, the atoms and molecules within the material gain kinetic energy, causing them to move more vigorously and occupy a greater amount of space. These materials that show expansion on heating are called positive thermal expansion (PTE) materials and have a positive value of thermal expansion coefficient. There also exists however a few materials that are known to contract, or exhibit a negative coefficient of thermal expansivity (NTE) [17].This phenomenon has been shown to occur in solids including complex metal oxides, polymers and zeolites. The existence of PTE and NTE materials and studying their properties opens the door to composites with a

19

coefficient of thermal expansion (CTE) of zero. These are materials that do not expand nor contract when there is a change in temperature. Understanding the principles of thermal expansion and its practical applications is crucial for designing and constructing various structures and devices that can withstand the effects of temperature changes.

Figure 2.8: Thermal expansion Set-up

Chapter 3

Discussion and Results

3.1 Results

3.1.1 X-ray Diffraction

The temperature dependent x-ray diffraction data is recorded in Fig **?? ??** and **??**.the data was taken in the ranges of $20 \leq 2\theta \leq 80$ at RT and were plotted using Lebail method.

The lattice parameters and space groups are given in the table 3.1 $MnCoGe_{1-x}Sn_x$ for $x = 0$ is found to be orthorhombic having space group $Pnma$. $MnCoGe_{0.925}Sn_{0.075}$ shows hexagonal peaks with no mixed phases. $MnCoGe_{0.9}Sn_{0.1}$ and $MnCoGe_{0.925}Sn_{0.075}$ are found to belong to space group $P63/mmc$, both being hexagonal.

	a	b	c	α	β	γ	Space group
$MnCoGe$	5.980179	3.827151	7.052467	90	90	90	$Pnma$
$MnCoGe_{0.925}Sn_{0.075}$	4.106574	4.106574	5.336641	90	90	120	$P63/mmc$
$MnCoGe_{0.9}Sn_{0.1}$	4.110355	4.110355	5.34548	90	90	120	$P63/mmc$

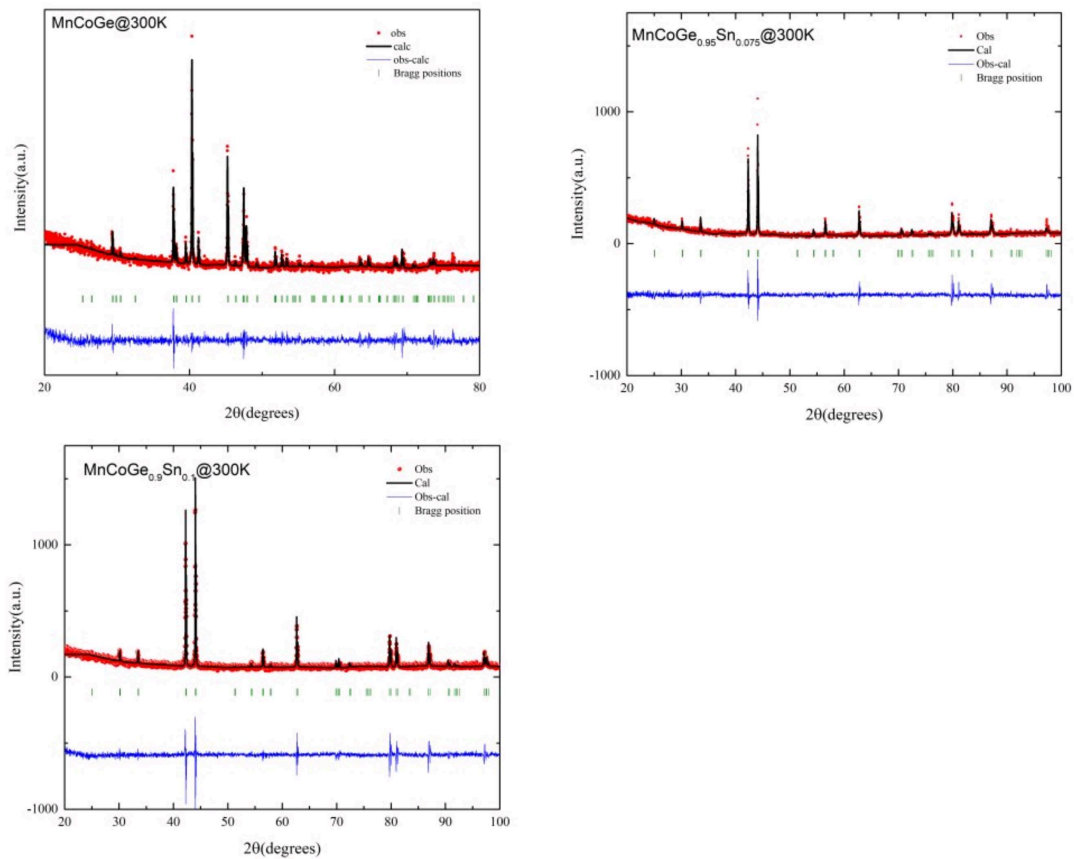Table 3.1: Lattice parameters and space groups

Figure 3.1: X-ray diffraction data for the alloys x=0 x=0.075 and x=0.1 at 300K.

3.1.2 Electrical Resistivity Measurements

Four probe resistivity was conducted on $MnCoGe_{0.95}Sn_{0.075}$ and $MnCoGe_{0.9}Sn_{0.1}$ given in fig3.1.2 and 3.1.2. The temperature range is from 50K to 400K. A slope change is observed at a temperature coinciding to the magnetic transition temperature reported in literature. Another change in slope is noticed at temperature below the magnetic transition temperature for $x = 0.075$. This change in slope below magnetic transition temperature is subtle for $x = 0.1$ sample. These are highlighted in fig3.1.2 and 3.1.2.

Figure 3.2: The temperature dependence of the normalized resistance during warming and cooling cycles and magnified view between the temperature ranges 50-200 for the alloy composition x=0.075
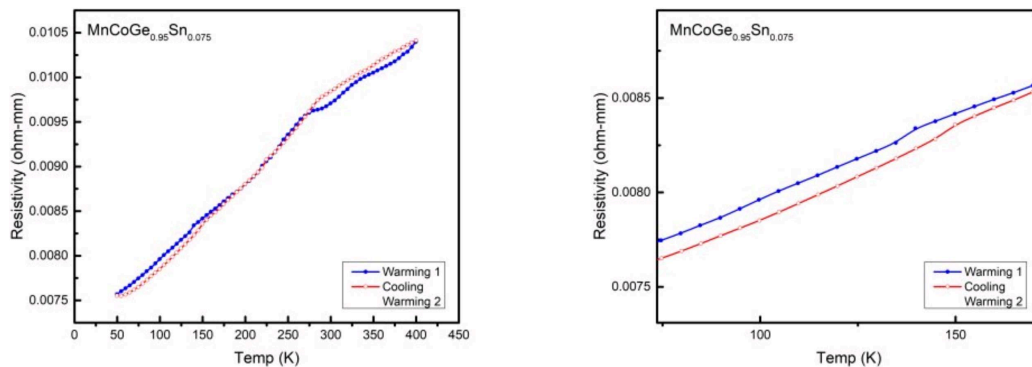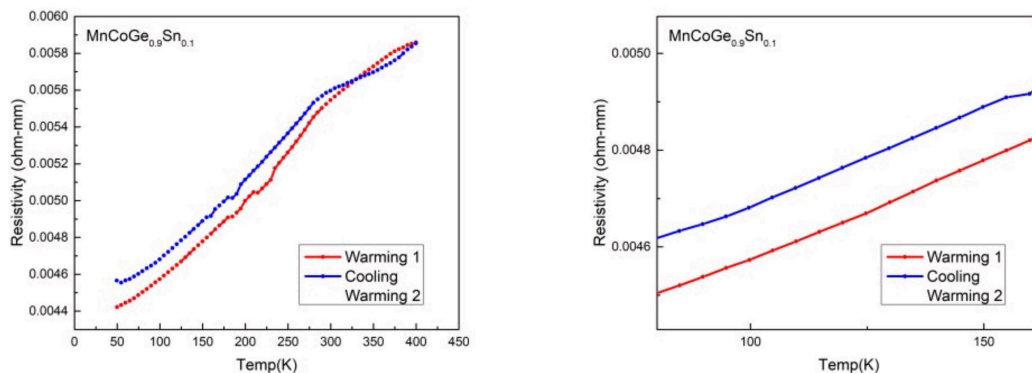

Figure 3.3: The temperature dependence of the normalized resistance during warming and cooling cycles and magnified view between the temperature ranges 50-200 for the alloy composition x=0.1.

3.1.3 DSC

Differential Scanning Calorimetry (DSC) mearsurements were done for the sample $MnCoGe$ is given in fig3.4. This was done to determine the martensitic transformation temperature for the alloy. The temperatures taken were from $250-450K$. The martensitic transformation temperature T_M was noted to be around 345K.
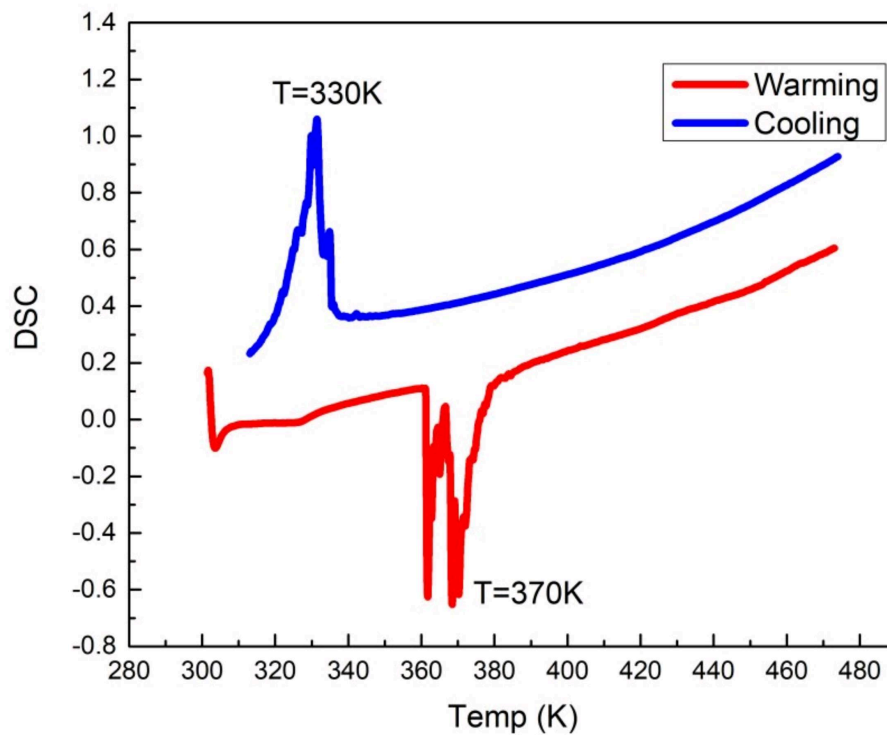

Figure 3.4: The thermo-analytical measurements showing DSC plot as a function of temperature for x=0.

3.1.4 Thermal Expansion Measurements

Thermal expansion measurements were conducted on $MnCoGe_{0.95}Sn_{0.075}$ and $MnCoGe_{0.9}Sn_{0.1}$ as can be seen from the fig3.1.4 and fig3.1.4. Coefficients of thermal expansion are

calculated. $MnCoGe_{0.95}Sn_{0.075}$ has a negative coefficient of thermal expansion $\alpha_1 = -2.77 \times 10^{-6}$ from 80K to 110K and later has $\alpha_2 = 0.305 \times 10^{-6}$ for temperatures above 110K. $x = 0.1$ sample has $\alpha_1 = -9.47 \times 10^{-6}$ between 75-120K and has $\alpha_2 = 2.35 \times 10^{-6}$ between 120K to 300K
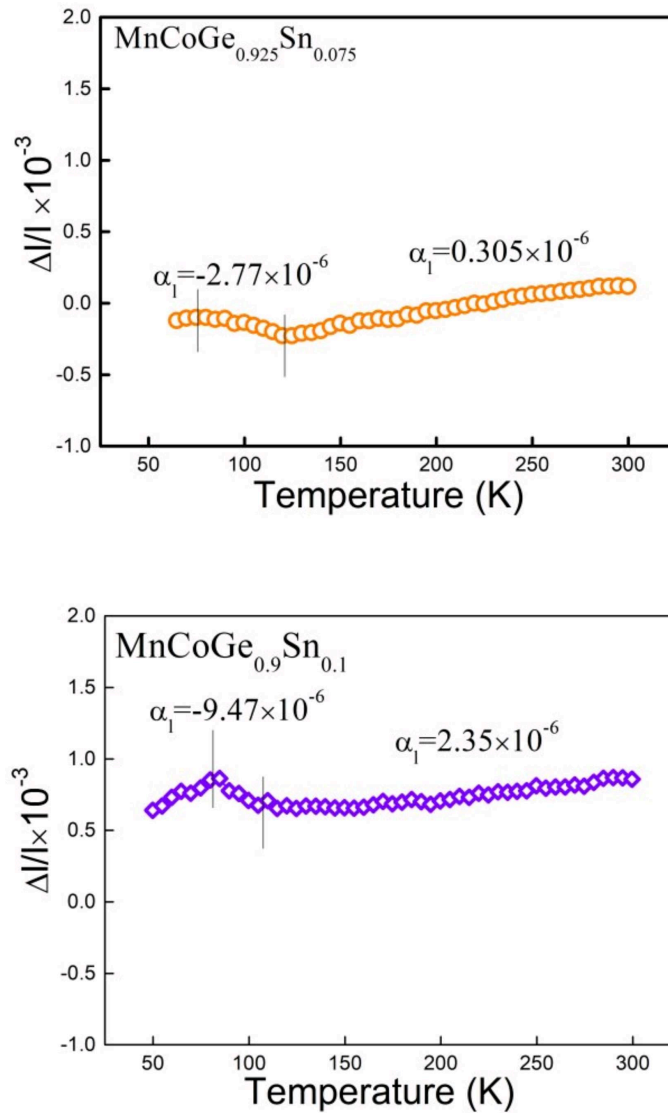

Figure 3.5: The temperature dependent thermal expansion measurements for the alloy compositions x=0.075 and x=0.1.

3.2 Discussion

The attempt of this study was to understand the martensitic transformation in $MnCoGe$ and to study the effects on this transformation when the stoichiometry is changed. Tin was added to the half heusler to create $MnCoGe_{1-x}Sn_x$ and the additional compositions of $x = 0.075$ and $x = 0.1$ were studied. From the X-ray diffraction data we see that $MnCoGe$ is in orthorhombic phase at room temperature indicating that a martensitic transformation has occurred. This is further clarified in the DSC plot which provides a clearer incite into the transition temperature. We also see that $x = 0.075$ and $x = 0.1$ are hexagonal at room temperature, which is the same phase as the parent structure. Hence we can infer that no structural phase transition has occurred. A change in slope can be observed in the resistivity data for $x = 0.75$ at a temperature coinciding to the magnetic transition temperature as reported in literature. This can also be seen for $x = 0.1$. The study of electrical resistivity also indicates another transition below the magnetic transition temperature for $MnCoGe_{0.95}Sn_{0.075}$ and $MnCoGe_{0.9}Sn_{0.1}$. However it appears to be more subtle in the $x = 0.1$ sample. An attempt was made to study the frequency response to strain at different temperatures however due to the brittle nature of the sample this method was unsuccessful. This transition was further studied by thermal expansion measurements to understand the effect of temperature on the strain of the material. The data supports the transitions observed in the electrical resistivity study. $MnCoGe_{0.95}Sn_{0.075}$ at low temperatures shows negative thermal expansion how ever at $T = 110K$ the material has a small positive coefficient of thermal expansion, indicating towards the possibility of Zero thermal expansion. $x = 0.1$ sample also changes from a NET to a PTE material.

The absence of a phase transition for the tin dopped alloys and the presence of a magnetic ordering at low temperatures is an interest to be further pursued.

Bibliography

[1] J. Dai, *Ferroic Materials for Smart Systems.* City, Country (if applicable): Springer, 2020.

[2] P. K. Kumar, *Shape Memory Alloys.* City, Country (if applicable): Publisher, Year.

[3] "Transformation twinning and deformation twinning of niti shape memory alloy," *Materials Science and Engineering: A*, vol. 660, pp. 1–10, 2016.

[4] D. C. Lagoudas, *Shape memory alloys: modeling and engineering applications.* Springer, 2008.

[5] A. R. Pelton, T. Duerig, and D. Stöckel, "A guide to shape memory and superelasticity in nitinol medical devices," *Minimally invasive therapy & allied technologies*, vol. 13, no. 4, pp. 218–221, 2004.

[6] G. Liu, J. Chen, Z. Liu, X. Dai, G. Wu, B. Zhang, and X. Zhang, "Martensitic transformation and shape memory effect in a ferromagnetic shape memory alloy: Mn2niga," *Applied Physics Letters*, vol. 87, no. 26, 2005.

[7] Y. Ge, O. Heczko, O. Söderberg, and V. Lindroos, "Various magnetic domain structures in a ni–mn–ga martensite exhibiting magnetic shape memory effect," *Journal of Applied Physics*, vol. 96, no. 4, pp. 2159–2163, 2004.

[8] K. Otsuka and K. Shimizu, "Pseudoelasticity and shape memory effects in alloys," *International Metals Reviews*, vol. 31, no. 1, pp. 93–114, 1986.

[9] K. Otsuka and K. Shimizu, "Pseudoelasticity and shape memory effects in alloys," *International Metals Reviews*, vol. 31, no. 1, pp. 93–114, 1986.

[10] Y. Long, Z. Zhang, D. Wen, G. Wu, R. Ye, Y. Chang, and F. Wan, "Phase transition processes and magnetocaloric effects in the heusler alloys nimnga with concurrence of magnetic and structural phase transition," *Journal of applied physics*, vol. 98, no. 4, 2005.

[11] G. Li, E. Liu, H. Zhang, Y. Zhang, J. Chen, W. Wang, H. Zhang, G. Wu, and S. Yu, "Phase diagram, ferromagnetic martensitic transformation and magnetoresponsive properties of fe-doped mncoge alloys," *Journal of magnetism and magnetic materials*, vol. 332, pp. 146–150, 2013.

[12] T. Gao, M. Wu, N. Qi, T. Zhou, X. Luo, Y. Liu, K. Xu, V. V. Marchenkov, H. Dong, Z. Chen, *et al.*, "Giant low field magnetocaloric effect and magnetostructural coupling in mncoge1-xinx around room temperature," *Journal of Alloys and Compounds*, vol. 753, pp. 149–154, 2018.

[13] V. Johnson, "Diffusionless orthorhombic to hexagonal transitions in ternary silicides and germanides," *Inorganic chemistry*, vol. 14, no. 5, pp. 1117–1120, 1975.

[14] Bruker Corporation, "X-ray diffraction (xrd) - bruker," Year of Publication/Access.

[15] L. B. Valdes, "Resistivity measurements on germanium for transistors," *Proceedings of the IRE*, vol. 42, no. 2, pp. 420–427, 1954.

[16] F. Nix and D. MacNair, "The thermal expansion of pure metals: copper, gold, aluminum, nickel, and iron," *Physical Review*, vol. 60, no. 8, p. 597, 1941.

[17] W. Miller, C. Smith, D. Mackenzie, and K. Evans, "Negative thermal expansion: a review," *Journal of materials science*, vol. 44, pp. 5441–5451, 2009.